PNAS
www.pnas.org

# Supplementary Information for

**Essential role of the oxytocin system for adaptive mate choice in both sexes**

Saori Yokoi, Kiyoshi Naruse, Yasuhiro Kamei, Satoshi Ansai, Masato Kinoshita, Mari Mito, Shintaro Iwasaki, Shuntaro Inoue, Teruhiro Okuyama, Shinichi Nakagawa, Larry J. Young, Hideaki Takeuchi

Dr. Saori Yokoi
Email: yokois@pharm.hokudai.ac.jp

Dr. Hideaki Takeuchi
Email: takeuchi@okayama-u.ac.jp

**This PDF file includes:**



**Other supplementary materials for this manuscript include the following:**





www.pnas.org/cgi/doi/10.1073/pnas.1921446117

# Methods

### TILLING and high-resolution melting curve experiments

This procedure was performed as previously described (1, 2). To amplify the *oxt* locus that includes the final gene product, we performed PCR with *oxt*-specific primers: 5'-TTTCTTCCTTTCTCTTCTTTTAATACC -3' and 5'-TTCCAAATTCAAGGAAAGGCT -3' using KOD-Plus (TOYOBO, Japan). The PCR conditions were as follows: 1 cycle of 94°C for 2 min, followed by 45 cycles of 94°C for 15 s, annealing at 58°C and then at 68°C for 30 s, and a final denaturing and re-annealing step (1 cycle of 94°C for 30 s, followed by rapid cooling to 28°C). Each of the 5771 PCR products derived from genomic DNA was subjected to a high-resolution melting assay. Based on differences in the melting curves, mutant candidates were selected. Melting curves were analyzed using the LightScanner (Idaho Technology, Salt Lake City, UT, USA). The mutations were then identified by sequencing the PCR product of the second positive genomic DNAs using BigDye Terminator version 3.1 (Applied Biosystems, Foster City, CA, USA) and the ABI 3730XL sequencing platform. We backcrossed the TILLING mutants with Cab fish three times and crossed those fish to generate the homozygous mutants.

### TALEN experiment

To generate *oxtr1*$^{-/-}$ mutants, TALEN experiments were performed as described previously (3). Potential TALEN target sites in the locus were searched using the TALEN Targeter program (https://tale-nt.cac.cornell.edu/node/add/talen). TAL repeats were assembled using the Golden Gate assembly method with slight modifications. Expression vectors for the TALENs were linearized by digestion with *NotI*. Capped RNAs were synthesized using the mMessage mMachine SP6 Kit (Life Technologies, Gaithersburg, MD, USA) and purified using the RNeasy Mini Kit (Qiagen, Valencia, CA, USA). Pairs of RNA for the TALENs (150 ng/$\mu$l) were injected into fertilized eggs of the drR strain and cab strain by a microinjection method.

### CRISPR/Cas9 experiment

Expression plasmids for sgRNAs were constructed by cloning the annealed oligonucleotides into pDR274 (Addgene Plasmid 42,250) (4). The target sequence for *oxtr1*$^{-/-}$ is 5'-GATATAACATGCAGAGCACACGG-3' and that for *oxtr2*$^{-/-}$ is 5'-TTTTACTTGAGCTGGAAAGTTGG-3'. The sgRNAs were transcribed from the DraI-digested template plasmids using the Ampliscribe T7-Flash Transcription Kit (Epicentre, Madison, WI, USA). Capped Cas9 mRNA was synthesized from linearized pCS2 + hSpCas9 (Addgene Plasmid 51,815) using the mMessage mMachine SP6 Kit (Thermo Fisher Scientific, Waltham, MA, USA). All synthesized RNAs were purified using the RNeasy Mini Kit (Qiagen, Hilden, Germany). Cas9 mRNA (100 ng/$\mu$l) and custom-designed sgRNA (25ng/ul) were mixed and injected into fertilized eggs of the drR strain by a microinjection method.

**RT-PCR**

Total RNA was extracted from the medaka brain (2 males or 2 females) using TriZol LS reagent (#10296010, Invitrogen). cDNA was synthesized using ReverTra Ace qPCR RT Master Mix with gDNA remover (TOYOBO, Japan). The resulting cDNA was used as a template for amplifying the *oxtr1* and *oxtr2* loci by Quick Taq HS DyeMix (TOYOBO, Japan) with *oxtr1*-specific primers: 5'- CAGTGCATTAACCTGACGCCCAAA-3' and 5'- GAATTGAAATCTCGCTCGCAGC-3' and *oxtr2*-specific primers: 5'-GGAGAGATCGCTTTGTAGCTGTC-3' and 5'- TGTTCATCACAGCCACAGGAAG-3'. As each forward primer was designed based on exon 1 and each reverse primer was designed based on exon 2, the estimated amplified products were not derived from the genome, but from mRNA. The PCR conditions were as follows: 1 cycle of 94°C for 1 min, followed by 35 cycles of 94°C for 30 s: annealing at 58°C and then at 68°C for 30 s. Amplified products were sequenced and PCR products were confirmed to derive from each mRNA.

**Prediction of secondary structure of oxtrs**

We obtained the genomic sequence information of *oxtr1* and *oxtr2* from the Ensemble medaka genome browser (http://www.ensembl.org/Oryzias_latipes/Info/Index) and predicted their secondary structure using "SOSUI", which is a program that predicts

transmembrane regions from amino acid sequences (http://harrier.nagahama-i-bio.ac.jp/sosui/sosui_submit.html).

**Female mating receptivity test**

To quantify the motivation of a female to mate with a male of interest, a female mating receptivity assay was performed as previously described (5). The day before the assay, males and females were separated in the evening (20:00-21:00) using two methods ("visual familiarization group" and "no visual familiarization group"). The next morning (10:00-12:00), the divider was removed and the male was placed into the tank with the female and mating behavior was recorded for 5 min. On the basis of video recordings, we determined the timing of the male quick-circle courtship displays and crossings (wrapping), followed by spawning. We calculated and compared the interval between the first male courtship behavior and the crossing followed by spawning in each group (latency to mate). The latency to mate negatively correlates with female mating receptivity.

**Mate-guarding test**

To determine whether males exhibited mate-guarding behavior, a mate-guarding test was performed as previously described (6). One female and two males (all male pairs were size-matched) were placed in the tank and their behavior was recorded from the bottom of the tank in the morning (10:00-12:00). As a negative control group (merged group), we performed the same experiment using virtually merged trios, recording one female and two males one by one, each placed in a separate aquarium. The male whose mean distance from the female was shorter than that of the other male was "the near male" and the other was "the far male". Based on the positions of the three fish, the angles between the vectors from the near male to the female and from the near male to the far male were calculated and the probability of those angles being obtuse was defined as the "guarding index". The significantly higher guarding indices of near males in the experimental groups compared with those in the merged groups indicate that the near males in the experimental groups exhibited mate-guarding.

### *In situ* hybridization

*In situ* hybridization of frozen brain sections was performed as described previously (7). The *oxtr1* cDNA fragment was amplified with forward primer 5′-**ATGGAGATCATTTCCAATGAAAGTGAG**-3′ and reverse primer 5′-**CATGTGGTGGAAGTCTGAGTAATGC**-3′ using synthesized cDNA as a template. Template cDNA was synthesized from mRNA extracted from the medaka brain using ReverTra Ace qPCR RT Master Mix with gDNA Remover (TOYOBO, Japan). Amplified *oxtr1* cDNA was subcloned into the pCR2.1 TOPO vector (Thermo Fisher Scientific, USA). The digoxigenin (DIG)-labeled riboprobes were synthesized from this plasmid by T7 or SP6 polymerase with a DIG labeling mix (Roche Diagnostics, Switzerland).

### Proximity test

To assess the interest of WT females toward *oxt*$^{I22F/I22F}$, *oxt*$^{-/-}$, and *oxtr1*$^{-/-}$ males, we performed a proximity test as previously described (8) with minor modification (SI Appendix, Fig. S6A). The WT female was placed into the inside tank (10-cm-diameter tank) and the male was placed into the outside tank (15-cm-diameter). After 1 min, we video recorded them for 1 min. From a series of frames, the position of the fish was extracted using the software UMATracker (http://ymnk13.github.io/UMATracker/) and the mean distance between two fish was calculated. For negative controls, position data of each fish was shuffled and virtually merged. If the inside fish have interest in the outside fish, the distance between them becomes significantly shorter than that for negative controls. Previously, our group showed that the interest of an outside fish toward an inside fish did not significantly affect the distance between them (8).

### OMR

We assessed the optomotor response of the *oxt*$^{I22F/I22F}$, *oxt*$^{-/-}$, and *oxtr1*$^{-/-}$ fish as previously described (9) (SI Appendix, Fig. S5A). The medaka were placed in a fixed 15-cm-diameter circular tank, which was placed within a striped 20-cm-diameter cylinder. The depth of water in the tank was 2 cm. The striped cylinder was positioned on a rotatable disk that was driven by a motor that could move in either direction and at various speeds. We recorded the optomotor response of medaka using a video camera from the bottom of

the tank and extracted the position of the medaka and stripes. A series of frames was analyzed using the software UMATracker (http://ymnk13.github.io/UMATracker/).

**RNA-seq and data analyses**

Whole brains from two adult females or males for one sample were homogenized in saline and TriZol LS reagent (#10296010, Invitrogen) was used to extract the total RNA. RNA-seq libraries were made using a Ribo-Zero Gold rRNA Removal Kit (H/M/R) (Illumina), TruSeq Stranded mRNA Library Prep kit (Illumina), and TruSeq RNA Single Indexes Set A and SetB (Illumina), according to the manufacturers' protocols. Sequencing was performed on the Illumina Hiseq 4000. Sequence reads were mapped to the medaka genome using HISAT2 (10). The numbers of sequence reads uniquely mapped to each exon were counted using featureCounts (11) on Ensembl annotation (ASM223467v1) with the -O option (allowMultiOverlap) and analyzed at the gene level. Omitting low-expressed genes (RPKM < 1.0) in WT fish, the count data were analyzed using DESeq2 (12) with the Wald test to determine which genes were significantly differentially expressed between WT and mutant fish (FDR < 0.05). To identify oxt system-regulated genes in a sex-specific manner, genes with FDR > 0.05 and $\log_2$ fold-change > 1.0 were removed for subsequent analyses because those genes were considered non-regulated genes due to sampling variation. For GO and Pathway analyses, ensemble IDs of medaka genes were converted to those of zebrafish homologs using BioMart and analyzed with GO-MWU (13) and PANTHER, respectively (14).

**Statistical analysis**

In the female mating preference test, the latency to mate in the visual familiarization group was compared with that in the no visual familiarization group using the Mann-Whitney *U*-test implemented in Statcel (OMS Ltd.). To examine the effect of *it* mutation on male courtship activity, we compared the numbers of courtship behaviors of WT, $oxt^{+/I22F}$, and $oxt^{I22F/I22F}$ males toward SF or non-SF females using Kruskal-Wallis and Steel-Dwass's post-hoc test implemented in the R system. To analyze the effect of SF on the motivation for courtship in $oxt^{I22F/I22F}$ males, we compared the number of courtship behaviors before SF with that after 7-8 days, 9-10 days, and 19-20 days of SF using Kruskal-Wallis

and Steel's post-hoc test implemented in R system. To examine whether the motivation for courtship toward unfamiliar females was different from that toward familiarized females, we compared the number of courtship behaviors before and that after SF using the Mann-Whitney *U*-test implemented in Statcel (OMS Ltd.). To determine whether males exhibited mate-guarding (mate-guarding test), we compared the guarding index of males of each genotype in the experimental groups with that of the negative control using the Mann-Whitney *U*-test implemented in Statcel (OMS Ltd.). In the dominance test, we compared the guarding index of two males using the Wilcoxon Signed-Ranks test implemented in Statcel (OMS Ltd.) and judged which male was dominant in each group. All p values are two-tailed.

A

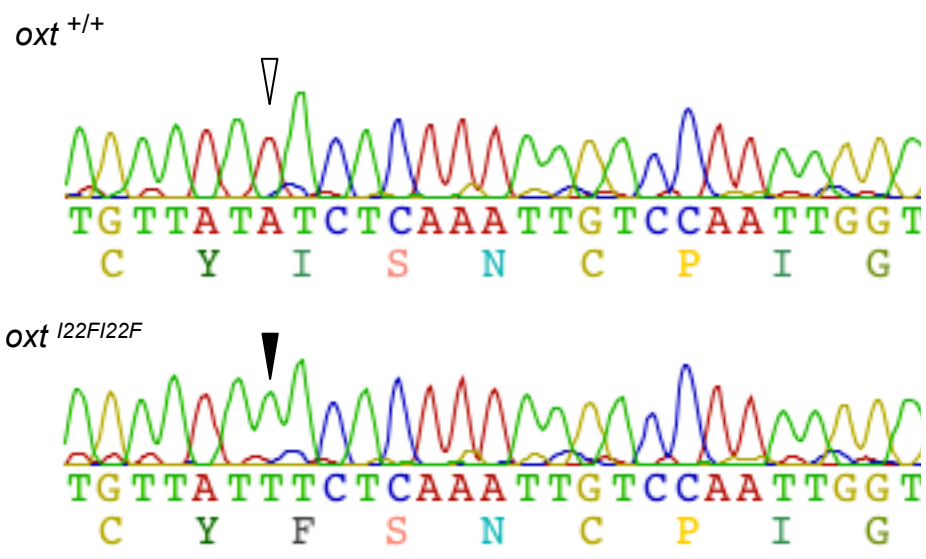


B

| species | gene | Amino acid sequence | | | | | | | | |
|---|---|---|---|---|---|---|---|---|---|---|
| mouse | *oxt* | C | Y | I | Q | N | C | F | L | G |
| chicken | bird *oxt* | C | Y | I | Q | N | C | P | I | G |
| fugu | fish *oxt* | C | Y | I | S | N | C | P | I | G |
| medaka | fish *oxt* | C | Y | I | S | N | C | P | I | G |
| medaka | *oxt*$^{I22F}$ | C | Y | F | S | N | C | P | I | G |

**Fig. S1. Screening for *oxt* mutants by TILLING methods.** (A) A local sequence dataset comparing the WT, *oxt* (*oxt*$^{+/+}$) and *oxt*$^{I22F}$ (*oxt*$^{I22F/I22F}$) homozygous mutants showing the *oxt* A66T mutation in *oxt*$^{I22F/I22F}$ (black arrowhead). (B) The primary structures of oxt homologs in vertebrates. All peptides are composed of 9 amino acids. Isoleucine 20, which is identical among oxt homologs, was changed to phenylalanine in the *oxt*$^{I22F}$ mutant allele (red letters).

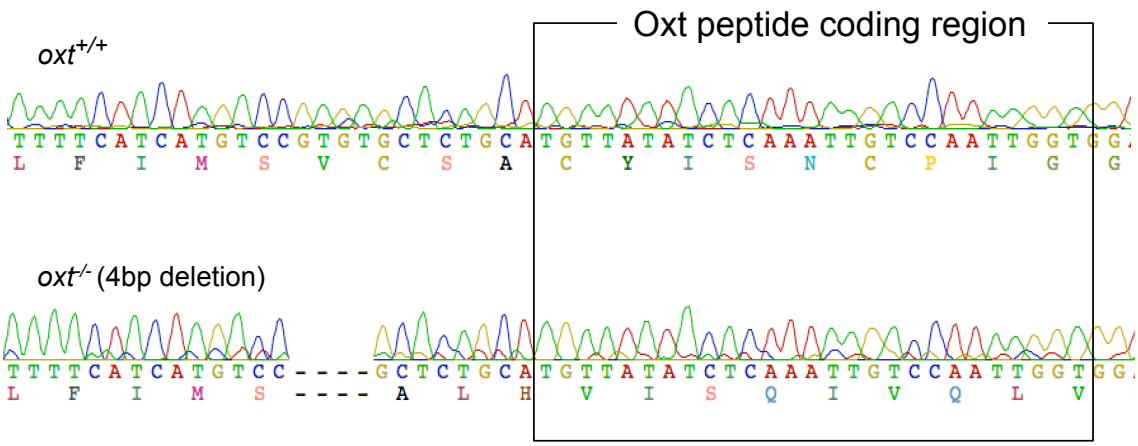


**Fig. S2. Generation of *oxt*$^{-/-}$ mutant by TALEN methods.** A local sequence dataset comparing the WT, *oxt* (*oxt*$^{+/+}$) and *oxt*$^{-/-}$ homozygous mutants demonstrating that a 4-bp deletion generated a frameshift of sequences that encode the oxt peptide.

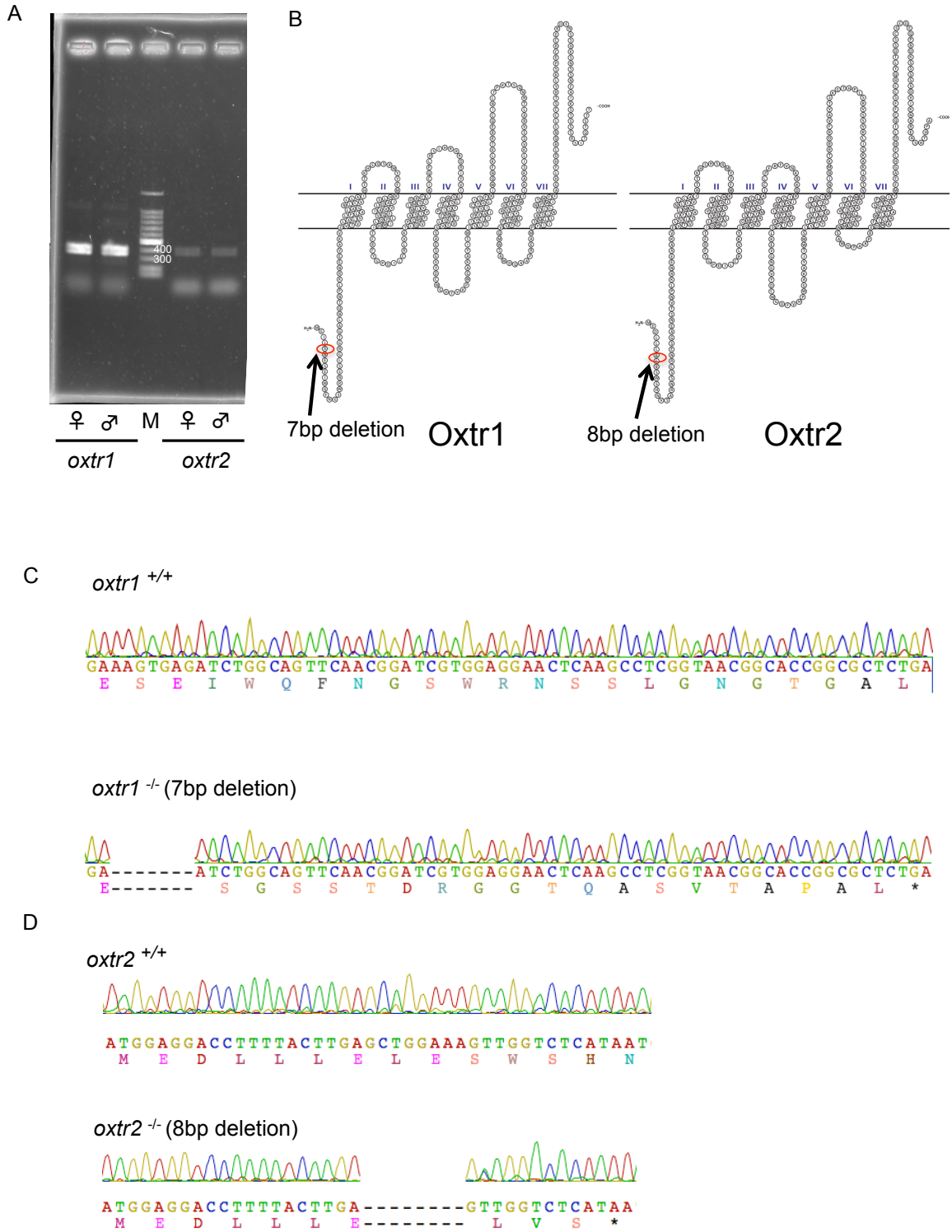


**Fig. S3. Generation of *oxtr1* and *oxtr2* mutants.** (A) RT-PCR analysis of *oxtr1* and *oxtr2* in the adult medaka brain. *oxtr1* and *oxtr2* mRNA was detected in brains of both sexes. Their estimated product sizes on the basis of PCR amplification were 368bp and 361bp, respectively. M: 100bp DNA ladder (Takara, Japan). As forward primers were

designed in exon1 and reverse primers were designed in exon2, these PCR products were amplified not from genomes, but from cDNAs. (B) Predicted secondary structures of oxtr1 (left) and oxtr2 (right). *oxtr1*$^{-/-}$ and *oxtr2*$^{-/-}$ have a 7-bp and an 8-bp deletion, respectively, in the first exon. (C) A local sequence dataset comparing the WT *oxtr1* (*oxtr1*$^{+/+}$) and *oxtr1*$^{-/-}$ homozygous mutants, indicating that a 7-bp deletion generated a nonsense mutation (G27X) in *oxtr1*$^{-/-}$. (D) A local sequence dataset comparing the WT *oxtr2* (*oxtr2*$^{+/+}$) and *oxtr2*$^{-/-}$ homozygous mutants, indicating that an 8-bp deletion generated a nonsense mutation (S12X) in *itr2*$^{-/-}$.

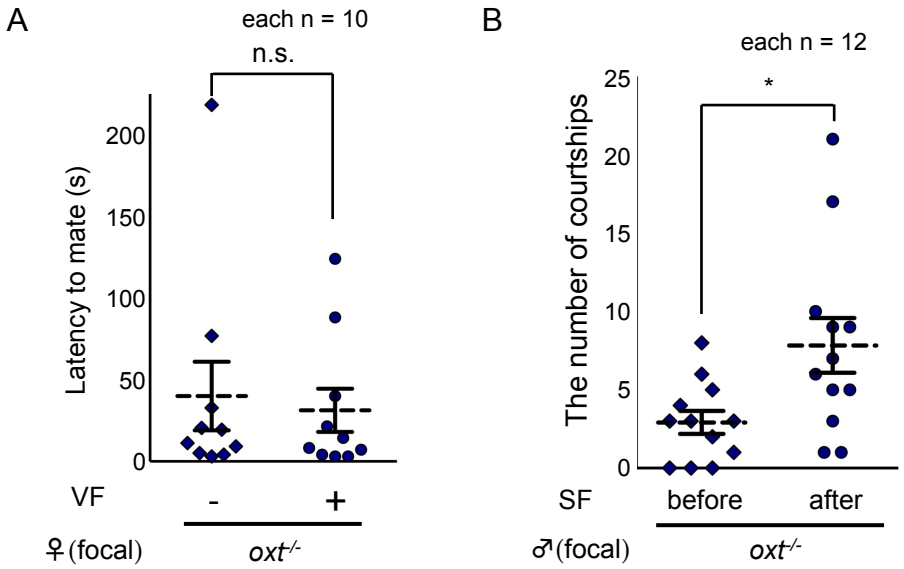


**Fig. S4. Female mate preference and male courtship behavior of *oxt*$^{-/-}$ mutants.** (A) In *oxt*$^{-/-}$ females, the latency to mate with unfamiliar males was as short as that with socially familiarized males. Mean ± SEM. n = 10/group, Mann-Whitney *U*-test. (B) The number of courtship behaviors of *oxt*$^{-/-}$ males was significantly increased by social familiarization. Mean ± SEM. n = 12/group,, Mann-Whitney *U*-test: $*P < 0.05$.

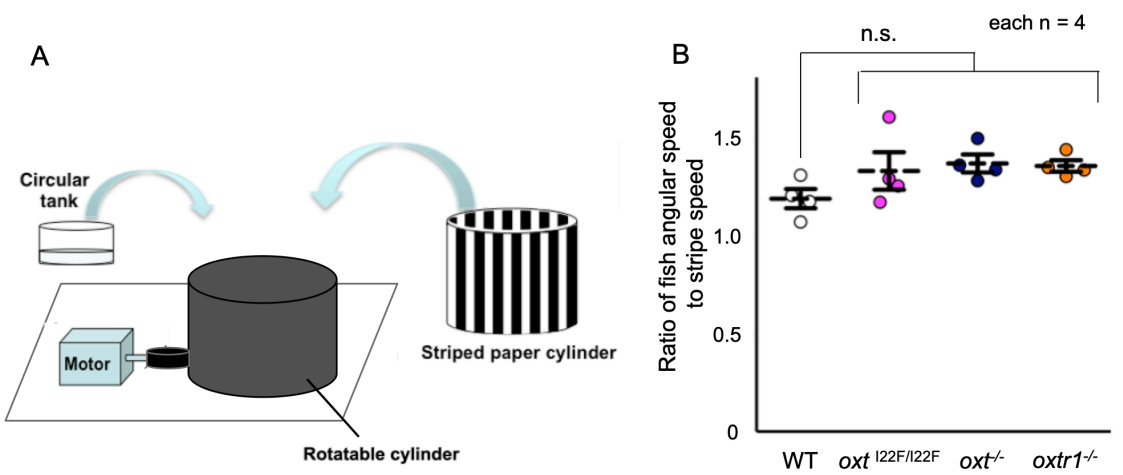


**Fig. S5. No significant defect of the optomotor response in *oxt*$^{I22F/I22F}$, *oxt*$^{-/-}$, and *oxtr1*$^{-/-}$ male fish.** (A) The apparatus used for the optomotor response test. (B) Ratio of the mean fish angular speed to the mean stripe speed of WT, *oxt*$^{I22F/I22F}$, *oxt*$^{-/-}$, and *oxtr1*$^{-/-}$ male fish. Mean ± SEM. n = 4/group, Kruskal-Wallis test.

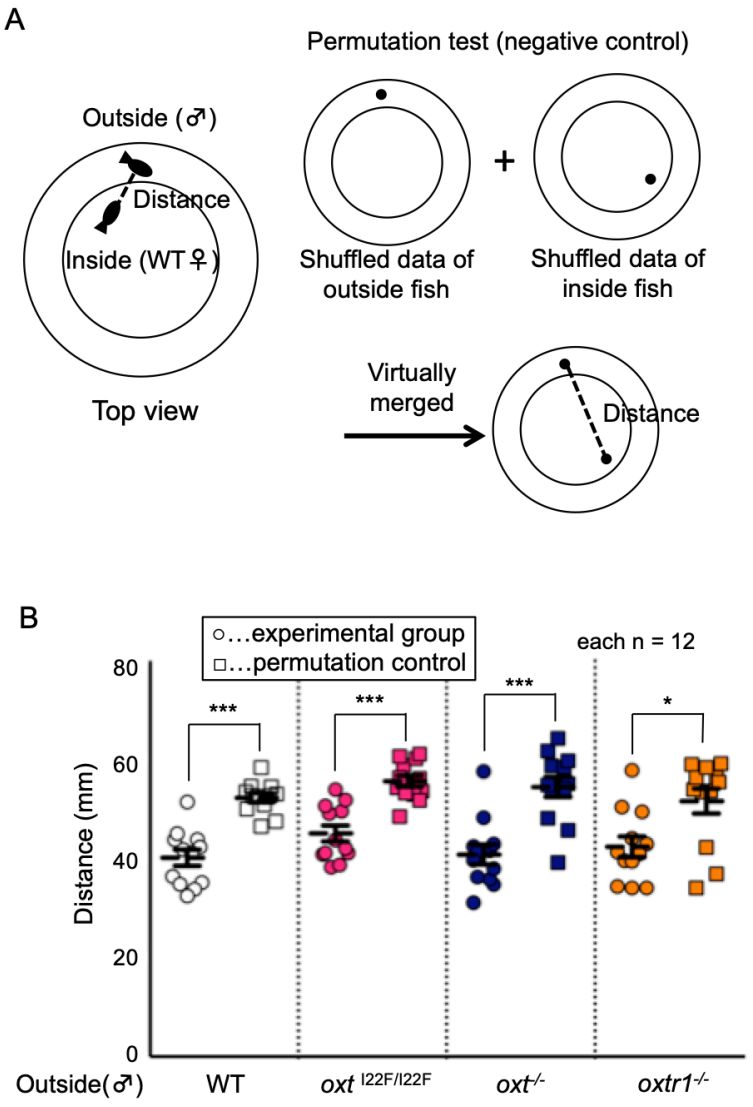


**Fig. S6. Normal proximity behavior of WT females, even toward mutant male fish.** (A) Assay scheme of the proximity test for assessing the interest of wild-type (WT) females toward mutant males. The WT female was placed into the inside tank and the male was placed into the outside tank. The distance between two fish was calculated. For negative controls, the position data of each fish were shuffled and virtually merged. (B) WT females exhibited normal interest, even toward *oxt*$^{I22F/I22F}$, *oxt*$^{-/-}$, and *oxtr1*$^{-/-}$ males. Mean ± SEM. n = 12/group, Mann-Whitney *U*-test: **P* < 0.05, ****P* < 0.001.

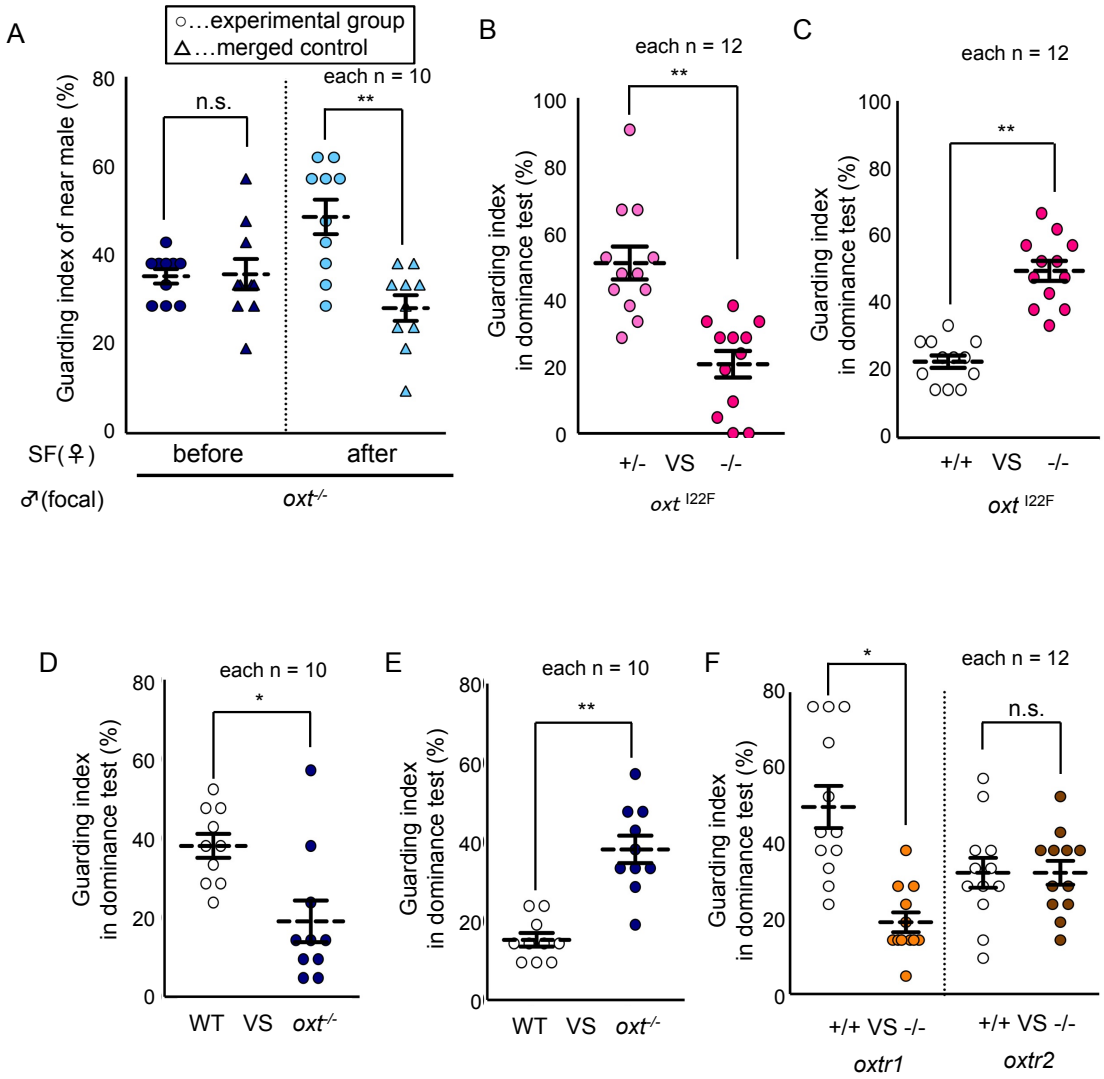


**Fig. S7. Mate-guarding behavior assay using *oxt*, *oxtr1*, and *oxtr2* mutant males.** (A) (A) While *oxt*$^{-/-}$ males did not exhibit mate-guarding behavior toward unfamiliar WT females, they exhibited mate-guarding toward socially familiarized WT females. Mean ± SEM. n = 10/group, Mann-Whitney *U*-test: $^{**}P < 0.01$. (B) *oxt*$^{I22F/I22F}$ males tended to be subordinate when unfamiliar females were used in the dominance test. Mean ± SEM. n = 12/group, Mann-Whitney *U*-test: $^{**}P < 0.01$. (C) When WT males and *oxt*$^{I22F/I22F}$ males had to compete for the familiar female, *oxt*$^{I22F/I22F}$ males tended to be dominant. Mean ± SEM. n = 12/group, Mann-Whitney *U*-test: $^{**}P < 0.01$. (D) *oxt*$^{-/-}$ males tended to be subordinate when unfamiliar females were used in the dominance test. Mean ± SEM. n = 10/group, Mann-Whitney *U*-test: $^{*}P < 0.05$. (E) When WT males and *oxt*$^{-/-}$ males competed for the familiar female, *oxt*$^{-/-}$ males tended to be dominant. Mean ± SEM. n = 10/group, Mann-Whitney *U*-test: $^{**}P < 0.01$. (F) When unfamiliar females were used in the dominance test, *oxtr1*$^{-/-}$ males tended to be subordinate, but there was no significant difference in dominance between WT males and *oxtr2*$^{-/-}$ males. Mean ± SEM. n = 12/group, Mann-Whitney *U*-test: $^{*}P < 0.05$.

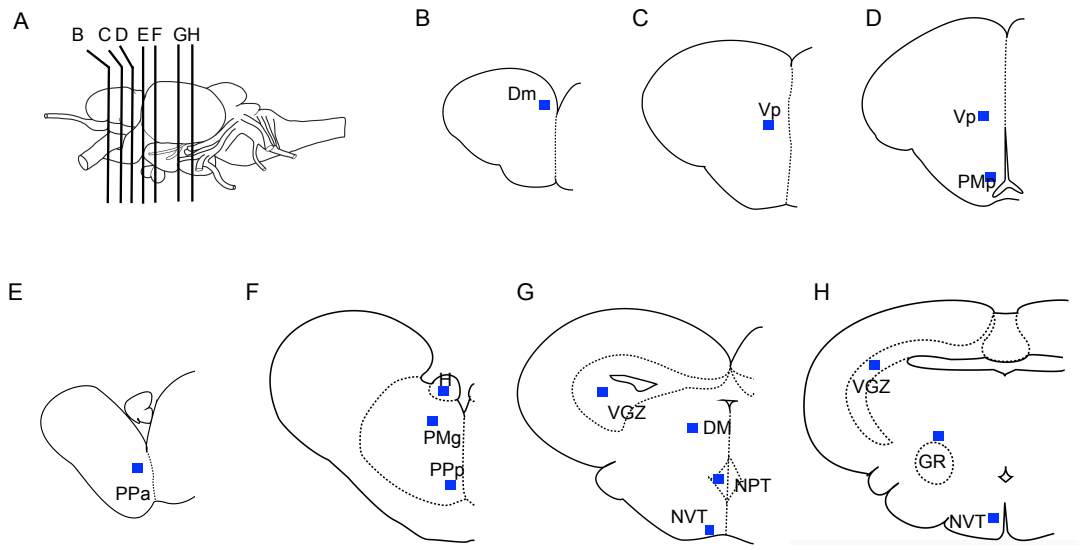
A
B C D E F GH
B
Dm
C
Vp
D
Vp
PMp
E
PPa
F
H
PMg
PPp
G
VGZ
DM
NPT
NVT
H
VGZ
GR
NVT

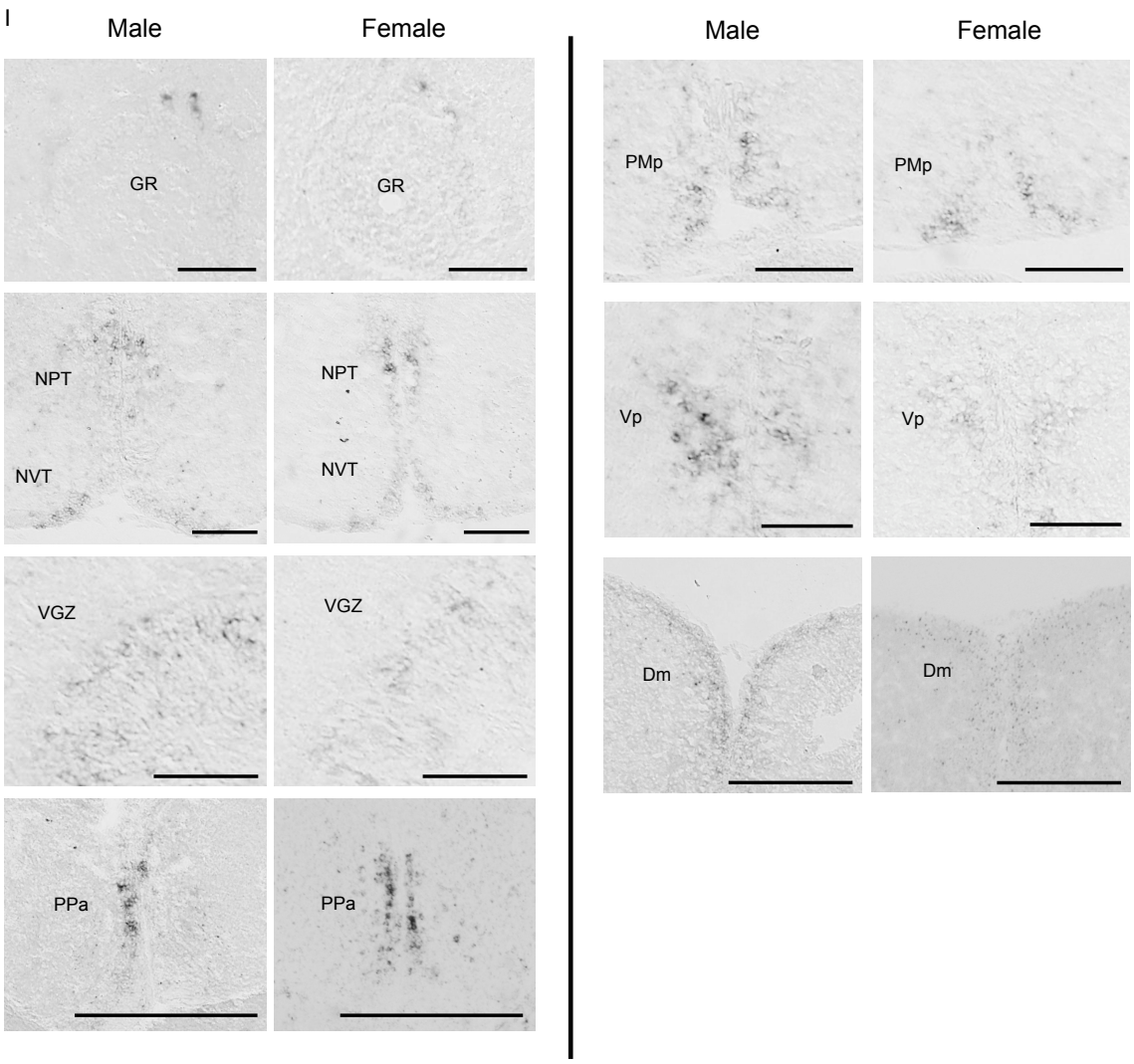
I
Male
Female
Male
Female
GR
GR
PMp
PMp
NPT
NVT
NPT
NVT
Vp
Vp
VGZ
VGZ
Dm
Dm
PPa
PPa

**Fig. S8. Distribution of *oxtr1*-expressing cells in the adult brain in both sexes.**
(A) Lateral view of the medaka brain. The positions of coronal sections B-H are indicated by the lines. (B-H) Schematic representation of *oxtr1*-expressing cell distribution (filled square). Dm: medial nucleus of the dorsal telencephalic area, Vp: posterior nuclei of the ventral telencephalic area, PMp: parvocellular portion of the magnocellular preoptic nucleus, PPa: anterior parvocellular preoptic nucleus, H: habenula, PMg: gigantocellular portion of the magnocellular preoptic nucleus, PPp: posterior parvocellular preoptic nucleus, VGZ: ventricular grey zone DM: nucleus dorsomedialis thalami NPT: nucleus posterior tuberis, NVT: nucleus ventral tuberis, GR: corpus glomerulosum pars rotunda. (I) Representative micrographs of *oxtr1*-expressing cells (left: male, right: female). All scale bars represent 100 μm.

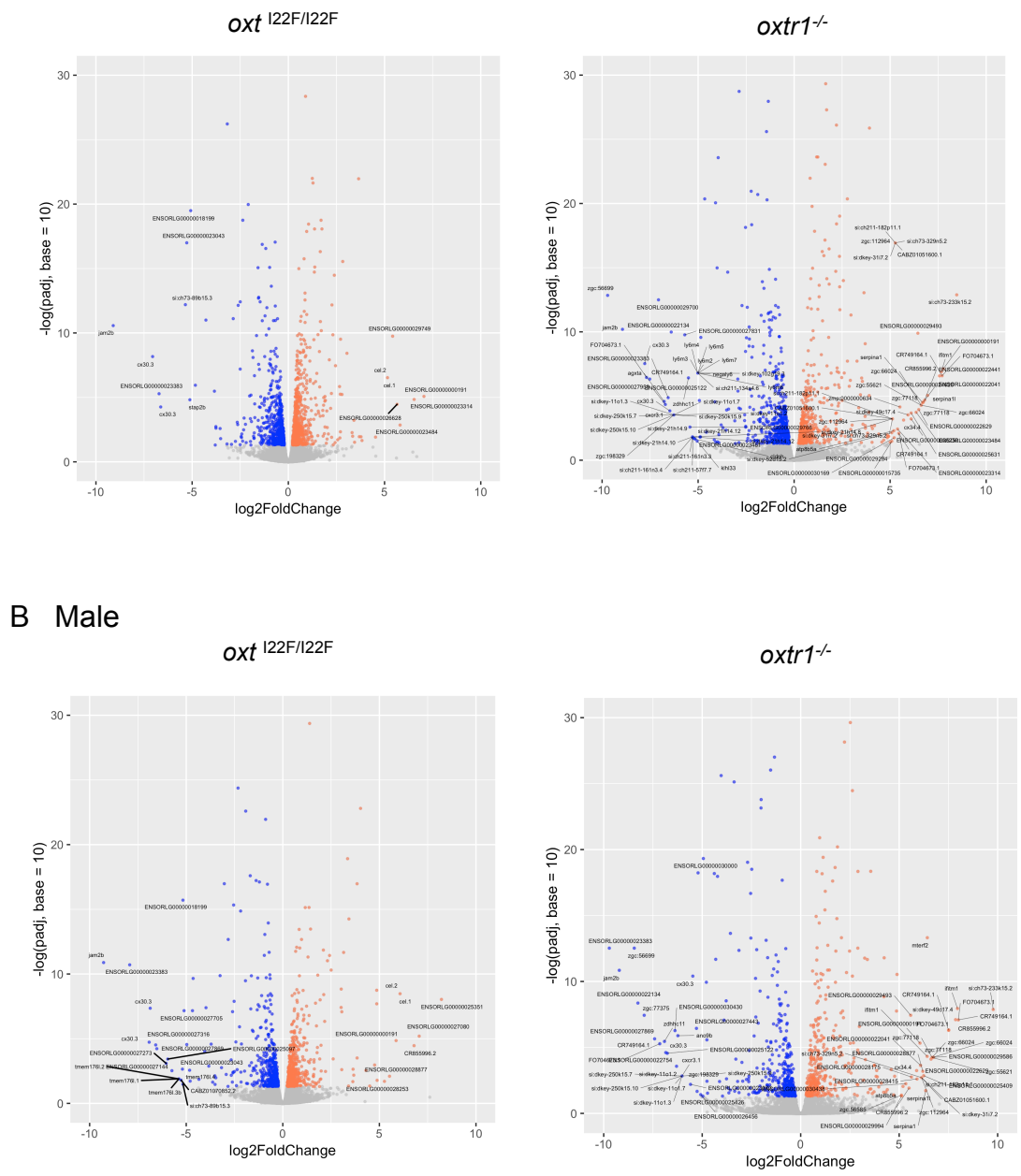


**Fig. S9. Volcano plots of upregulated/downregulated genes in *oxt* and *oxtr1* mutants.** Log2foldChange in gene transcription levels in female mutants (A) and male mutants (B) compared with those in WT fish. Each dot represents one gene. Gray dots indicate genes whose transcription levels were not significantly changed in mutants compared with those in WT (FDR>0.05). Orange and blue dots represent significantly upregulated/ downregulated genes in mutants, respectively. Names of highly upregulated/ downregulated genes (log2FoldChange < -5 or log2FoldChange > 5) are represented.

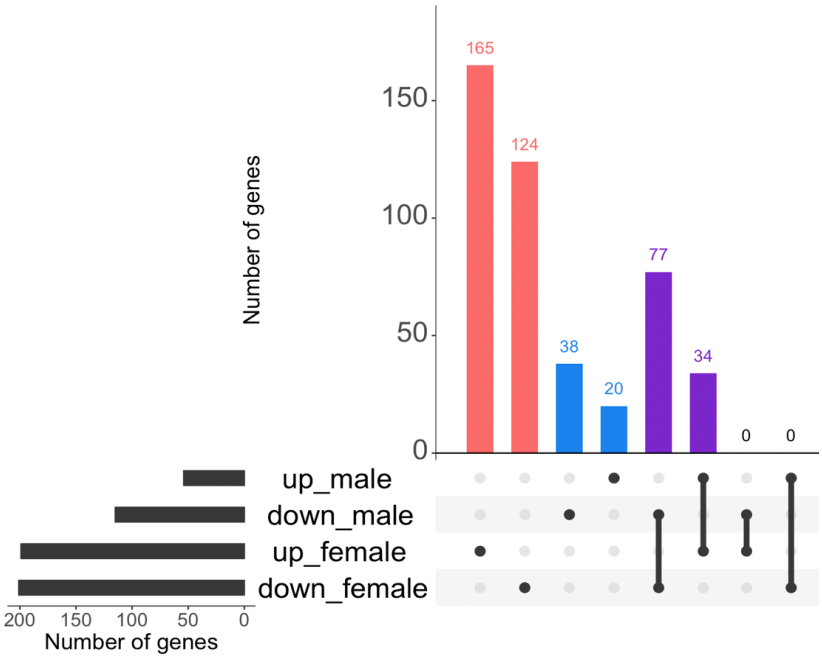


**Fig. S10. Number of genes upregulated/downregulated in mutants.** Purple bars indicate upregulated/downregulated genes in both sexes. Red bars indicate upregulated /downregulated genes only in females. Blue bars indicate upregulated/downregulated genes only in males. None of the genes were regulated oppositely between females and males.

A Upregulated 34 genes in both sexes (log2FC>0 & FDR<0.05 in 4 groups)

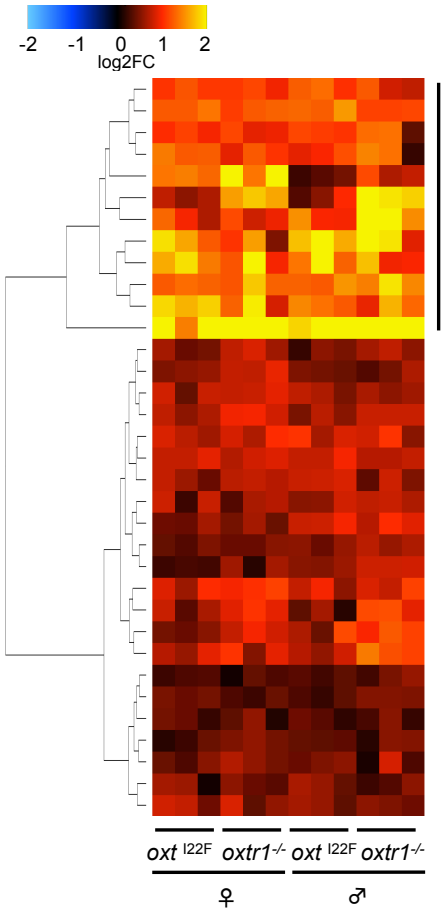


| Ensembl ID | Gene name |
|---|---|
| ENSORLG00000028232 | cyp2p7 |
| ENSORLG00000003379 | NSA2 ribosome biogenesis homolog |
| ENSORLG00000003685 | traf3ip2l |
| ENSORLG00000003673 | chd1l |
| ENSORLG00000003910 | si:dkey-183j2.10 |
| ENSORLG00000008103 | Centrosomal protein of 72 kDa |
| ENSORLG00000004500 | Phosphoglucomutase 5 |
| ENSORLG00000029699 | TRAF3-interacting protein 2-like |
| ENSORLG00000020644 | CD99 molecule |
| ENSORLG00000026471 | - |
| ENSORLG00000002982 | Fumarylacetoacetate hydrolase domain-containing 2A |
| ENSORLG00000015608 | Zgc:66449 |

GO analysis BP & Pathway analysis
No significant term

B Downregulated 77 genes in both sexes (log2FC<0 & FDR<0.05 in 4 groups)

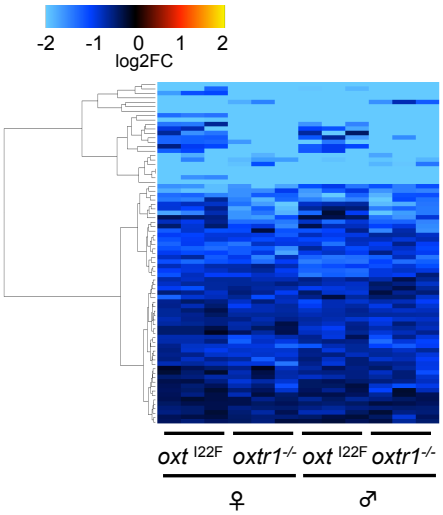


GO analysis BP

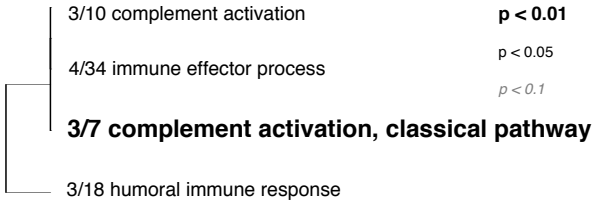


Pathway analysis

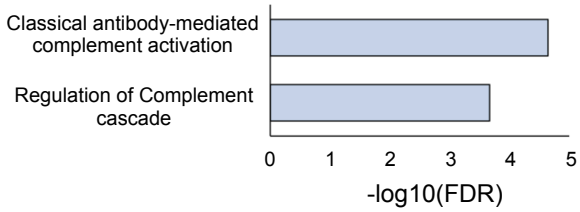

**Fig. S11. Upregulated/downregulated genes in both sexes of *oxt* and *oxtr1* mutants**
(A) Clustering analysis of 34 genes that were significantly upregulated in *oxt* and *oxtr1* mutants of both sexes. We did not detect enrichment of these genes for any terms. 12 genes that tended to be highly upregulated in mutants are listed next to the heatmap. There was no enrichment of these genes for any terms. (B) Clustering analysis of 77 genes significantly downregulated in *oxt* and *oxtr1* mutants of both sexes. GO and pathway analysis revealed enrichment of these genes for "complement activation, classical pathway". Each column represents the results of one sample (mixed RNA sample from two fish). Each gene was sorted by k-means cluster. The heatmap color means log2foldchange compared with WT.

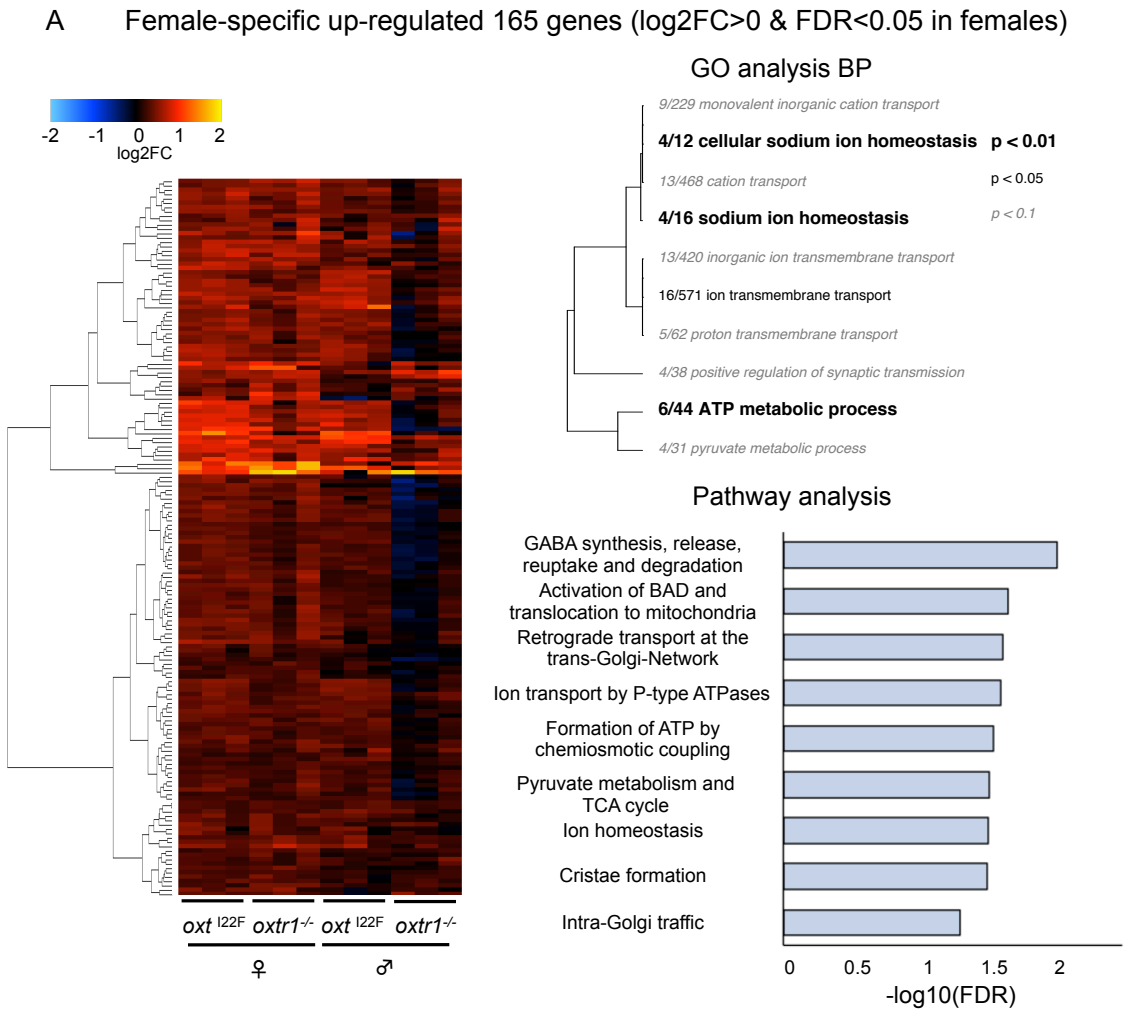

B Female-specific down-regulated 124 genes (log2FC<0 & FDR<0.05 in females)

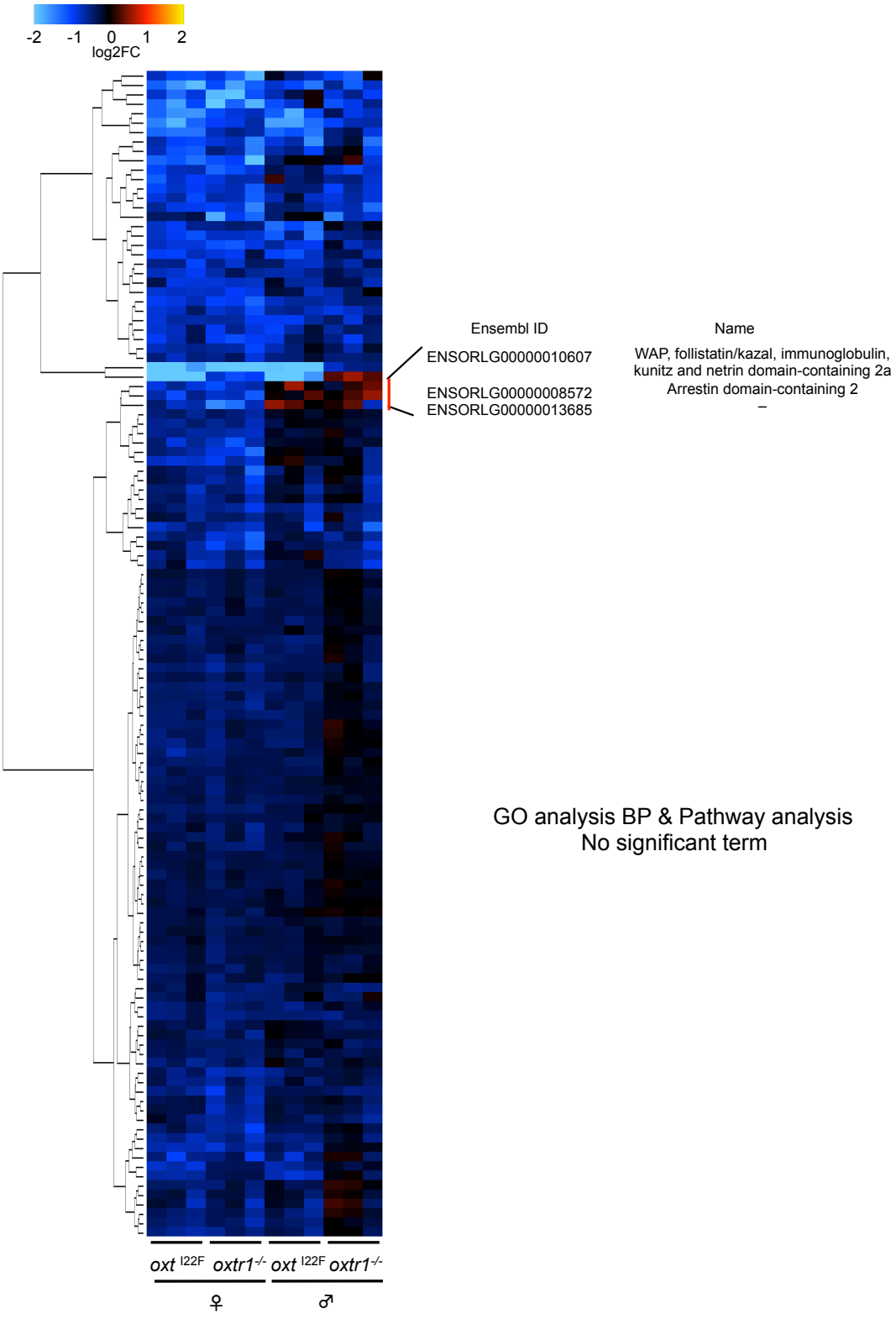


GO analysis BP & Pathway analysis
No significant term

**Fig. S12. Upregulated/Downregulated genes in female *oxt* and *oxtr1* mutants**
(A) Clustering analysis of 165 genes significantly upregulated only in female *oxt* and *oxtr1* mutants. GO analysis showed an enrichment of genes involved in cellular sodium ion homeostasis and ATP metabolic process. Each column represents the results of one sample (mixed RNA sample from two fish). (B) Clustering analysis of 124 genes that were significantly downregulated only in female *oxt* and *oxtr1* mutants. GO and Pathway analyses revealed no enrichment of these genes for any terms. Three genes that tended to be downregulated specifically in mutant females are listed next to the heatmap. There was no enrichment of these genes for any terms. Each column represents the results of one sample (mixed RNA sample from two fish). Each gene was sorted by k-means cluster. The heatmap color means log2foldchange compared with WT.

A Male-specific up-regulated 20 genes (log2FC>0 & FDR<0.05 in males)

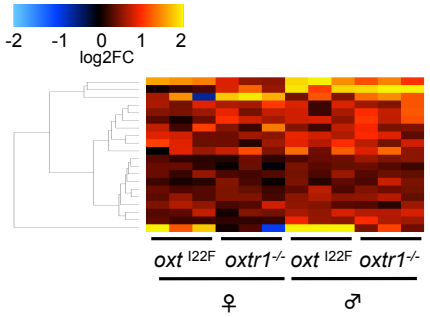


GO analysis BP… No significant term

Pathway analysis

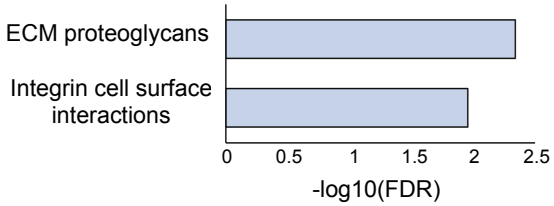


B Male-specific down-regulated 39 genes (log2FC<0 & FDR<0.05 in males)

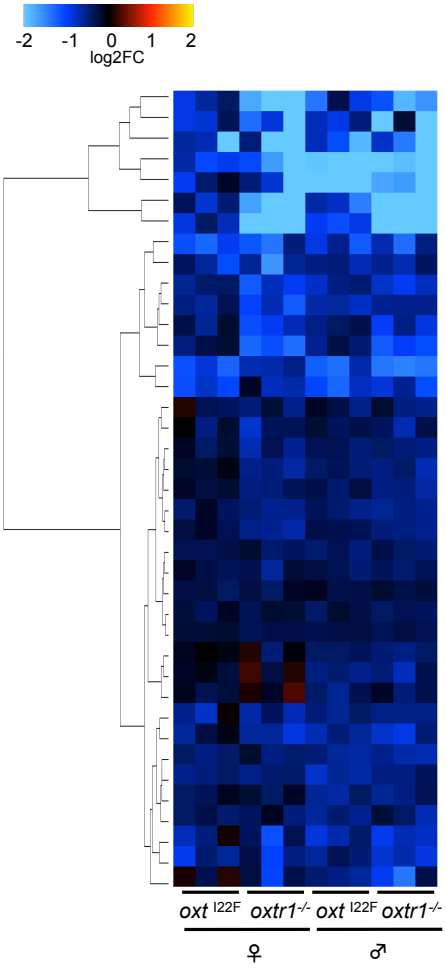


| Ensembl ID | Name |
|---|---|
| ENSORLG00000025661 | Zgc:91849 |
| ENSORLG00000005709 | ATPase, Cu++-transporting, alpha polypeptide |
| ENSORLG00000022228 | - |
| ENSORLG00000024569 | zgc:112966 |
| ENSORLG00000012369 | Homeobox protein Hox-B1b |
| ENSORLG00000026426 | Von Willebrand factor A domain-containing 7 |
| ENSORLG00000001254 | - |
| ENSORLG00000027859 | Tudor domain-containing 12 |
| ENSORLG00000010987 | Centromere protein F |
| ENSORLG00000025206 | Unc-13 homolog D |
| ENSORLG00000014333 | - |
| ENSORLG00000009014 | G patch domain and ankyrin repeats 1 |
| ENSORLG00000008841 | Transmembrane protein 67 |
| ENSORLG00000016794 | C3 and PZP-like, alpha-2-macroglobulin domain-containing 8 |
| ENSORLG00000006865 | Queuine tRNA-ribosyltransferase catalytic subunit 1 |
| ENSORLG00000024993 | Apolipoprotein A-II |
| ENSORLG00000009119 | Alpha-2-HS-glycoprotein 2 |
| ENSORLG00000013947 | Carboxylic ester hydrolase |
| ENSORLG00000007444 | Chimerin 2 |
| ENSORLG00000010222 | - |
| ENSORLG00000022640 | COP9 signalosome complex subunit 9 |
| ENSORLG00000013042 | Talin 1 |
| ENSORLG00000015864 | SREBF chaperone |
| ENSORLG00000003465 | Cytochrome P450 26B1 |
| ENSORLG00000020723 | Dihydropyrimidinase-like 4 |
| ENSORLG00000018708 | Si:dkey-49c17.3 |
| ENSORLG00000001595 | Phospholipid-transporting ATPase |
| ENSORLG00000016538 | Elongation of very long chain fatty acids protein 1 |
| ENSORLG00000008564 | DMalpha2b |
| ENSORLG00000027657 | Neurogenic differentiation factor 1 |
| ENSORLG00000014330 | Unc-51-like kinase 3 |
| ENSORLG00000008808 | Protein tyrosine phosphatase, receptor type, C |
| ENSORLG00000004597 | Beclin 1, autophagy-related |
| ENSORLG00000003575 | Peptidylprolyl isomerase |
| ENSORLG00000022325 | DNA-damage-inducible transcript 3 |
| ENSORLG00000015953 | Sodium/potassium-transporting ATPase subunit alpha |
| ENSORLG00000003884 | Spastic paraplegia 20a |
| ENSORLG00000002047 | Ammonium transporter Rh type B |
| ENSORLG00000015596 | Lysine-specific demethylase 7A |

GO analysis BP & Pathway analysis …No significant term

**Fig. S13. Upregulated/downregulated genes in male *oxt* and *oxtr1* mutants** (A) Clustering analysis of 20 genes that were significantly upregulated only in male *oxt* and *oxtr1* mutants. Pathway analysis revealed enrichment of these genes for "Extracellular matrix organization". (B) Clustering analysis of 39 genes significantly downregulated only in male *oxt* and *oxtr1* mutants. GO and Pathway analyses did not reveal enrichment of these genes for any terms. Each column represents the results of one sample (mixed RNA sample from two fish). Each gene was sorted by k-means cluster. The heatmap color means log2foldchange compared with WT.

**Table S1. Generated mutants in this study**

| Target gene | Mutation | Method |
|---|---|---|
| *oxt* | I22F | TILLING |
| *oxt* | 4bp deletion | CRISPR/Cas9 |
| *oxtr1* | 7bp deletion | TALEN |
| *oxtr2* | 8bp deletion | CRISPR/Cas9 |

**Movie S1. Mate-guarding movie using one *oxt*$^{+/I22F}$ male, one *oxt*$^{I22F/I22F}$ male and one unfamiliar female**

This movie is played at double speed. Two males are same with those in Movie S2.

**Movie S2. Mate-guarding movie using one *oxt*$^{+/I22F}$ male, one *oxt*$^{I22F/I22F}$ male and one familiar female**

This movie is played at double speed. Two males are same with those in Movie S1.

**Additional data table S1 (separate file)**

The list of upregulated/downregulated genes in *oxt* and *oxtr1* mutants.

**Additional data table S2 (separate file)**

The list of upregulated/downregulated genes in *oxt* and *oxtr1* mutants in a sex-specific manner and in a non sex-specific manner.

**Supplementary Reference**


1. Taniguchi Y, et al. (2006) Generation of medaka gene knockout models by target-selected mutagenesis. *Genome Biol* 7:R116.
2. Ishikawa T, et al. (2010) High-resolution melting curve analysis for rapid detection of mutations in a Medaka TILLING library. *BMC Mol Biol* 11:70. doi:10.1186/1471-2199-11-70.
3. Ansai S, et al. (2013) Efficient targeted mutagenesis in medaka using custom-designed transcription activator-like effector nucleases. *Genetics* 193:739–749.
4. Ansai S, Kinoshita M (2014) Targeted mutagenesis using CRISPR/Cas system in medaka. *Biol Open* 3:362–371.
5. Okuyama T, et al. (2014) A Neural Mechanism Underlying Mating Preferences for Familiar Individuals in Medaka Fish. *Science* 343:91–94
6. Yokoi S, et al. (2015) An essential role of the arginine vasotocin system in mate-guarding behaviors in triadic relationships of medaka fish (*Oryzias latipes*). *PLOS Genet* 11:e1005009.
7. Isoe Y, Okuyama T, Taniguchi Y, Kubo T, Takeuchi H (2012) p53 Mutation suppressed adult neurogenesis in medaka fish (Oryzias latipes). *Biochem Biophys Res Commun* 423:627-31.
8. Isoe Y, Konagaya Y, Yokoi S, Kubo T, Takeuchi H (2016) Ontogeny and Sexual Differences in Swimming Proximity to Conspecifics in Response to Visual Cues in Medaka Fish. *Zool Sci* 33:246-54.
9. Imada H, et al. (2010) Coordinated and Cohesive Movement of Two Small Conspecific Fish Induced by Eliciting a Simultaneous Optomotor Response. *PLoS ONE* 5:e11248.
10. Kim D, Langmead B, Salzberg SL (2015) HISAT: a fast spliced aligner with low memory requirements. *Nat Methods* 12:357–360.
11. Liao Y, Smyth GK, Shi W (2014) featureCounts: an efficient general purpose program for assigning sequence reads to genomic features. *Bioinformatics* 30:923–930.
12. Love MI, Huber W, Anders S (2014) Moderated estimation of fold change and dispersion for RNA-seq data with D ESeq2. *Genome Biol* 15. doi:10.1186/s13059-014-0550-8.
13. Wright RM, Aglyamova GV, Meyer E, Matz MV (2015) Gene expression associated with white syndromes in a reef building coral, Acropora hyacinthus. *BMC Genomics* 16:371.
14. Huaiyu M, Paul T. (2009) PANTHER Pathway: An ontology-based pathway database coupled with data analysis tools. *Protein Networks and Pathway Analysis 563,* eds Nikolsky Y, Bryant J (Humana Press), pp 123-140.